Intergranular Magnetoresistance in Sr_2FeMoO_6 from a Magnetic Tunnel Barrier Mechanism across Grain Boundaries

D. D. Sarma,[1,2,3,*] Sugata Ray,[1,4] K. Tanaka,[5] M. Kobayashi,[5] A. Fujimori,[5] P. Sanyal,[2] H. R. Krishnamurthy,[2,*] and C. Dasgupta[2,*]

[1]*Solid State and Structural Chemistry Unit, Indian Institute of Science, Bangalore 560 012, India*
[2]*Centre for Condensed Matter Theory, Department of Physics, Indian Institute of Science, Bangalore 560 012, India*
[3]*Centre for Advanced Materials, Indian Association for the Cultivation of Science, Kolkata 700 032, India*
[4]*Materials and Structures Laboratory, Tokyo Institute of Technology, Yokohama 226-8503, Japan*
[5]*Department of Physics and Department of Complexity Science and Engineering, University of Tokyo, Bunkyo-ku, Tokyo 113-0033, Japan*

(Received 24 April 2006; revised manuscript received 28 September 2006; published 12 April 2007)

We present magnetization (M) and magnetoresistance (MR) data for a series of Sr_2FeMoO_6 samples with independent control on antisite defect and grain-boundary densities, which reveal several unexpected features, including a novel switching-like behavior of MR with M. These, in conjunction with model calculations, establish that the MR in Sr_2FeMoO_6 is dominantly controlled by a new mechanism, derived from the magnetic polarization of grain-boundary regions acting like spin valves, leading to behavior qualitatively different from that usually encountered in tunneling MR. We show that a simple and useful experimental signature for the presence of this spin-valve-type MR (SVMR) is a wider hysteresis in MR compared to that in M.

DOI: 10.1103/PhysRevLett.98.157205 PACS numbers: 75.47.Gk, 72.25.−b, 75.60.−d

The recent discovery of magnetoresistance (MR) in polycrystalline Sr_2FeMoO_6, at considerably higher temperatures and lower magnetic fields [1] compared to colossal magnetoresistance (CMR) materials [2] like manganites, has generated a great deal of interest in view of its immense technological potential. Remarkably, the low-field MR is absent in single crystal samples [3], and so it has been suggested [3,4] that the MR here arises from tunneling magnetoresistance (TMR) between ferromagnetic metallic regions separated by insulating barriers.

Two alternative scenarios for the MR in Sr_2FeMoO_6 have been proposed. In one, physical grain boundaries are believed to provide intergrain tunnel barriers [5]; in the other, Fe/Mo antisite disorder (ASD), giving rise to antiferromagnetic, insulating Fe-O-Fe patches in between ferromagnetic metallic Sr_2FeMoO_6 islands within a single grain [4], is presumed to generate intragrain tunnel barriers. It is difficult to pick between these, as synthetic parameters [6], such as the annealing temperature, which change the Fe/Mo sublattice ordering and hence the density of antisite defects, also change the grain sizes, the average thickness, number or density of the grain boundaries, and possibly their chemical composition (depending on the oxygen partial pressure and temperature), all in an uncontrolled manner.

In this Letter, we present data on Sr_2FeMoO_6 samples where the two crucial parameters, namely, the antisite defect density and the grain-boundary density, are controlled independently, while keeping other physical properties essentially unchanged. We thereby show that the dominant mechanism of MR in Sr_2FeMoO_6 is from intergrain tunneling across physical grain boundaries. More importantly, several unique features in the experimental results and a comparison with simulations based on a realistic model Hamiltonian establish that the MR here is dominantly controlled by the magnetism of the grain boundaries acting like spin valves, in contrast to conventional TMR, and thereby defining a new type of MR, namely, spin-valve-type MR (SVMR).

Our samples, prepared by the arc melting method, were initially highly disordered as characterized by x-ray diffraction (XRD) [7]. By melting the reactants at around 2500 °C and resolidifying, samples (labeled A) with large-grains (10–20 μm) and relatively few grain boundaries, as confirmed by scanning electron microscopy (SEM), could be produced. We also prepared three other samples, B, C, and D, by annealing samples of type A for a period of 5 hours in 2% H_2/Ar atmosphere, at 1173 K, 1523 K , and 1673 K, respectively. SEM in conjunction with energy dispersive analysis of x-ray (EDX) revealed no change in the grain morphologies and composition due to this annealing process. However, the extent of the Fe/Mo ordering, quantified by $(I_{19.6°}/I_{32.1°})$ [1,7], the ratio of the intensity of the supercell (101) reflection at $2\theta = 19.6°$ to that of the normal reflection at $2\theta = 32.1°$, increased progressively for A, B, D, C, suggesting 1523 K as the optimal annealing temperature. Then, we took approximately half of each of A, B, C, and D, ground them finely to an average grain size of 2–3 μm and cold-pressed at room temperature to form samples A′, B′, C′ and D′, respectively. Samples in each pair (A, A′), (B, B′), (C, C′), and (D, D′) thus have the same antisite defect density but differ in grain sizes and grain-boundary density by an order of magnitude. Careful XRD, M(T) as well as spectro-microscopy experiments, establish

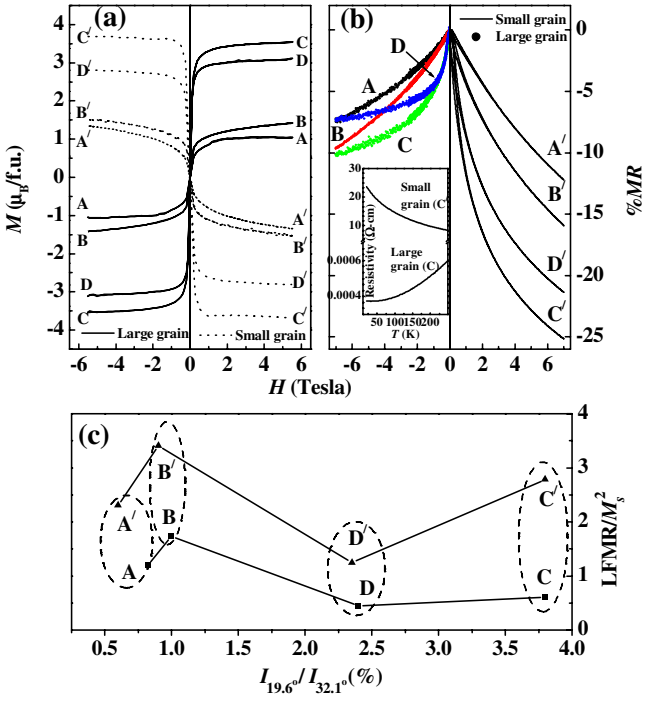

FIG. 1 (color online). (a) M(H) plots (solid lines) and -M(H) plots (dashed lines) for the large- and small-grain samples, respectively. (b) % MR(H) for the large-grain samples (solid circles, left half) and for the small-grain samples (lines, right half). Inset: Variation of resistivity with temperature for large- and small-grain samples with the same level of antisite defect densities. (c) Variation of the low-field MR (LFMR) normalized by M_s^2 with the extent of Fe/Mo ordering.

all the samples to be single phasic and homogeneous, similar to the ones discussed in [8].

In Fig. 1(a), we show the M(H) plots (solid lines) for the large-grain samples, A–D, and -M(H) plots (dashed lines) for the small-grain samples, A′–D′ (to avoid crowding of the data), all measured at 5 K. The saturation magnetization M_S for samples within each pair is very similar due to their identical antisite defect density, but M_S increases monotonically across both the series, i.e., with the extent of Fe/Mo ordering, consistent with antisite defects producing antiferromagnetic regions [9]. The resistivity (ρ) vs temperature (T) (shown for a sample pair (C, C′) in the inset to Fig. 1(b) of the large-grain samples are metallic, and very similar to that of single crystal samples [3], while the same for the small-grain samples are always several orders of magnitude larger and exhibit semiconducting behavior, suggesting that grain boundaries offer insulating barriers to macroscopic charge transport in these samples. Figure 1(b) shows the % MR $[=100\times[R(H,T)-R(0,T)]/R(0,T)]$ versus the magnetic field H at 20 K. For clarity and easy comparison, we have shown it for negative sweep of H for the large-grain samples (A–D), and for positive sweep of H for the small-grain samples (A′–D′). The % MR of the small-grain samples are uniformly several times larger than that of the corresponding large-grain samples, establishing that intergrain rather than intragrain tunneling processes, which gets strongly enhanced by the presence of large amount of grain boundaries, is the dominant contributor to the MR in these samples.

In further confirmation of this, Fig. 1(c) shows the low-field MR (LFMR) (extracted using the standard procedure [10,11] of drawing a tangent to the MR(H) plots at the highest field and finding its intercept on the MR axis), normalized by the squared saturation magnetization, as a function of $(I_{19.6^\circ}/I_{32.1^\circ})$. The change in normalized LFMR along either of the series ABDC or A′B′D′C′ (i.e., along solid lines in Fig. 1(c)) may be attributed solely to changes in ASD levels. On the other hand, the much larger (100–200%) enhancement of LFMR in going from a large-grain sample to the small-grain one at the same level of Fe/Mo ordering (ellipses in Fig. 1(c)), establishes that grain boundaries rather than antisite defects act as the primary tunnel barriers relevant for TMR in these samples. While enhancement of MR with decreasing grain size have been observed before [5,12], the antisite defect and grain-boundary concentrations had not been controlled independently.

We now demonstrate that the detailed magnetic field dependence of the MR in Sr_2FeMoO_6 is, however, not of the usual TMR or PMR [13] type. The MR(H) for typical TMR materials, such as CrO_2 [13,14], manganites [15], and Co-Cu alloys [16], show hysteresis with the sweep of the applied magnetic field H such that the peak in MR coincides with the corresponding coercive fields (H_c) in M(H). This is expected in case of conventional TMR, as the resistance is maximum when the net magnetization vanishes [17]. In striking contrast, the small-grain Sr_2FeMoO_6 intriguingly shows a peak in MR at an $H = \tilde{H}_c$ about 6 times larger than the corresponding H_c, as shown, for example, for the sample D′ in Fig. 2(a). We find that the value of $\tilde{H}_c$ is essentially the same for all the samples A′–D′, although their antisite defect densities, and consequently, the intragrain saturation magnetizations, differ strongly. In fact, the $\tilde{H}_c$ is invariably several times larger than H_c for all Sr_2FeMoO_6 samples we have studied so far. This suggests that intragrain properties are not the key determinants for this unexpected aspect of the MR. Further evidence of an unusual TMR is provided by the variation of the MR with M/M_s shown in Fig. 2(b); the inset to Fig. 2(b) shows that the MR is not proportional to $(M/M_s)^2$, as is expected for the usual TMR process [17,18]. Furthermore, Fig. 2(b) also shows that an applied field big enough to induce 80% of the saturation magnetization is still not enough to show a non-negligible MR. Instead, almost the entire MR is realized extremely rapidly for the last 20% of the magnetization, indicating that the tunneling process switches on only for an applied field much larger than the coercive field of the sample. Finally, as shown in the example in the inset to Fig. 2(a), the smaller grain samples show larger coercive fields in the M(H) plot (dashed line) compared to that of the corre-

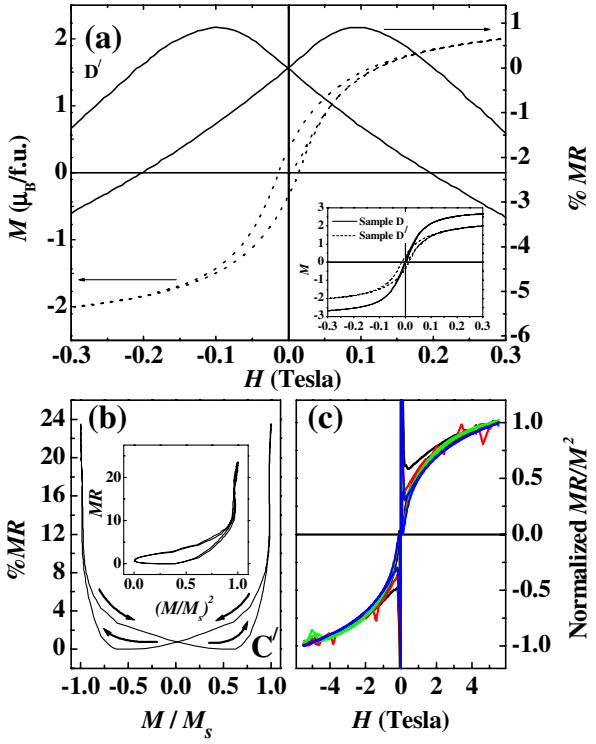

FIG. 2 (color online). (a) Comparison between the low-field variation of the MR and M in one illustrative case. Inset: Comparison of M(H) for a typical pair of large- and small-grain samples. (b) MR vs. M/M_s. Inset: MR vs $(M/M_s)^2$ (c) Normalized MR/M^2 curve as function of field for the small-grain samples.

sponding large-grain samples (solid line). These results suggest that the grain boundaries in our samples are hard magnets, with a higher coercive field than the bulk material, in contrast to the nonmagnetic [17] or antiferromagnetic [19] boundaries that have been considered in earlier work on TMR. These boundaries crucially control the tunneling processes and, therefore, the MR, although the bulk intragrain parts of the sample dominate the magnetization [20].

Further support to this "grain-boundary magnetism controlled MR" scenario is provided by the plot of MR/M^2 versus H for the four small-grain samples shown in Fig. 2(c). After scaling by the M^2 dependence [17,18] characteristic of standard TMR, we expect this normalized MR to be largely independent of intragrain properties. Instead, besides the artifact of this quantity blowing up as M^2 approaches zero, it still depends on H and shows a hysteresis loop. Furthermore, there is nearly a data collapse or universal hysteretic behavior, of the normalized MR for samples with widely different intragrain properties (extent of Fe/Mo ordering, density of antisite defects, and magnetization). This confirms that the MR is controlled not so much by the bulk magnetization M dominated by intragrain regions, but rather by the magnetic anisotropy properties of the grain-boundary regions.

To conclusively establish this scenario, we model the mobile Mo electrons moving in the background of Fe spins, approximated as classical spins, by the Anderson-Hasegawa [21] (AH) Hamiltonian. We simulate the tunneling geometry by considering a rectangular 10×3 array of spins on a square lattice, consisting of a single 10-spin column of "grain boundary" (GB) sandwiched between two 10-spin columns of "grains" (G), as shown schematically in Fig. 3(a). To make the GB insulating, we put a tunnel barrier by adding to the AH Hamiltonian site-diagonal terms at the sites of the GB. The difference that we have here compared to a standard simulation of TMR is the inclusion of the magnetism of the GB layer and its effect on transport. The z components of all the spins in both the "grains" are assumed to vary with the magnetic field H as the Langevin function $S_z = \coth(\alpha H) - \frac{1}{\alpha H}$, with α being treated as an adjustable parameter, but their x and y components, assumed to be the same for all spins within each grain, are allowed to fluctuate randomly over different realizations (as indicated by the cones defining the fixed z component in Fig. 3(a)), which are averaged over. We model and control the antisite disorder by making a fraction of the grain spins very stiff and randomly oriented, without aligning with H. The spins in the GB layer have random uniaxial anisotropy directions, marked by dashed short lines in Fig. 3(a), and are updated by a Monte Carlo algorithm. After each such update, the conductance of the itinerant electrons in the background of Fe spins is calculated by a standard Transfer Matrix method [22], and the result is averaged over 5000 GB spin configurations and 500 grain spin realizations for each value of H.

The results of our simulations, shown in Figs. 3(b)–3(f), agree excellently with the experimental ones in Figs. 1 and 2. For example, Fig. 3(b) shows the MR as a function of the applied field (made dimensionless by dividing by temperature [23]) for different numbers of antisite defects (cases P, Q, R, and S); the corresponding variation of the grain magnetization with the applied field is shown in Fig. 3(c). These resemble closely the experimental data in Figs. 1(a) and 1(b). Figure 3(d), showing an expanded region of the calculated MR data near zero field for the case P, illustrates the pronounced hysteresis effect in the MR, while the grain magnetization, also shown in the same panel, does not have any hysteresis by construction [24]. Figure 3(e) showing the calculated % MR vs M/M_s for the case P, and Fig. 3(f), the normalized MR/M^2 vs H for all cases, in turn match closely the corresponding experimental results shown in Figs. 2(b) and 2(c). The theoretical MR values are somewhat larger than the experimental ones for the same value of M_s, presumably because of the presence of alternative scattering mechanisms of nonmagnetic origin in real samples. If the different scattering rates are additive following Mattheisen's rule, the saturation value of MR is indeed expected to diminish.

In conclusion, we have shown that the MR in Sr_2FeMoO_6 is *predominantly intergrain rather than intra-*

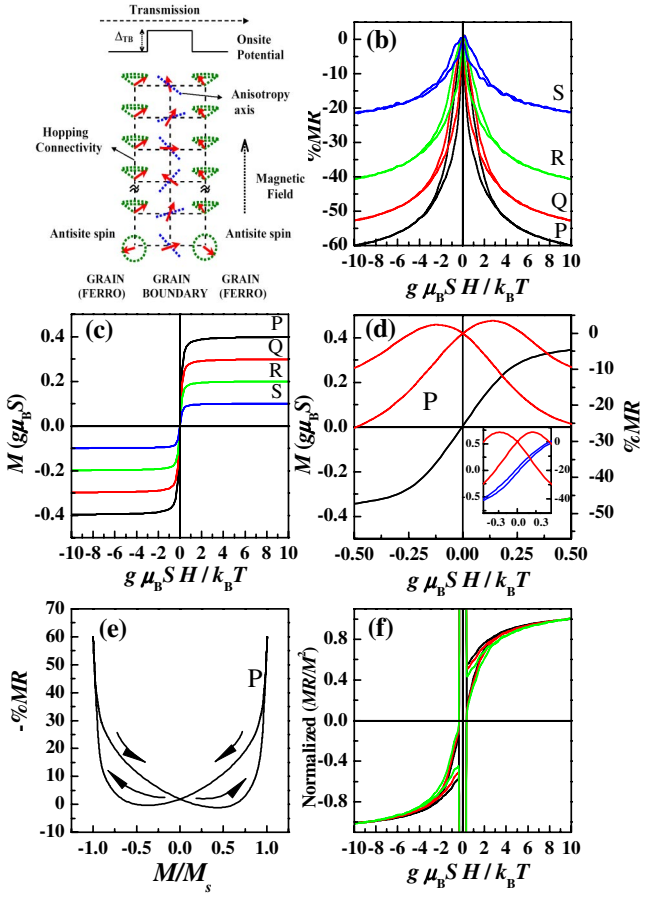

FIG. 3 (color online). (a) Schematic of the model used for the simulation. Fluctuating classical spins located at sites of a 10×3 lattice (dashed lines) on which itinerant electrons hop according to the AH Hamiltonian. Tunnel barrier $\Delta_{TB} = 10t$ (t = bare hopping), electron energy $E = 4t$, $E_{\text{anisotropy}}/k_BT = 4$. (b) and (c) Theoretical % MR(H) and M(H) curves, respectively, for 6(P), 7(Q), 8(R), and 9(S) antisite spins. (d) Low-field variation of the theoretical MR and M for the case P. Inset: see Ref. [24]. (e) MR vs M/M_s, for the case P. (f) Variation of normalized MR/M^2, with the applied field, for the cases P, Q, and R.

grain, due to tunneling across physical grain boundaries by a G-GB-G transport process. Additionally, we have shown that the MR has unusual features in its variation with the magnetization M and the applied field H, which can be understood by assuming that the grain-boundary region is not just insulating, but also *magnetic with a coercive field larger than that of the intragrain regions*. This leads to an MR, controlled or ''switched'' by the spin-polarization of the insulating barrier layer acting as a spin-valve. The experimental signature of such a spin-valve-type MR (SVMR) is a higher ''coercive'' field of the MR than that of the intragrain magnetization.

We thank the Department of Science and Technology and Board of Research in Nuclear Science, Government of India, for financial support.

*Also at Jawaharlal Nehru Centre for Advanced Scientific Research, Bangalore, India.

[1] K.-I. Kobayashi, T. Kimura, H. Sawada, K. Terakura, and Y. Tokura, Nature (London) **395**, 677 (1998).
[2] For reviews, see *Colossal Magnetoresistive Oxides*, edited by Y. Tokura (Gordon and Breach, London, 1999).
[3] Y. Tomioka *et al.*, Phys. Rev. B **61**, 422 (2000).
[4] M. García-Hernández, J. L. Martínez, M. J. Martínez-Lope, M. T. Casais, and J. A. Alonso, Phys. Rev. Lett. **86**, 2443 (2001).
[5] M. Venkatesan, C. B. Fitzgerald, U. V. Varadaraju, and J. M. D. Coey, IEEE Trans. Magn. **38**, 2901 (2002).
[6] L. Balcells *et al.*, Appl. Phys. Lett. **78**, 781 (2001).
[7] D. D. Sarma *et al.*, Solid State Commun. **114**, 465 (2000); D. D. Sarma, Curr. Opin. Solid State Mater. Sci. **5**, 261 (2001).
[8] D. Topwal *et al.*, Journal of Chemical Sciences **118**, 87 (2006).
[9] D. Topwal, D. D. Sarma, H. Kato, and Y. Tokura, Phys. Rev. B **73**, 094419 (2006).
[10] H. Y. Hwang and S. W. Cheong, Science **278**, 1607 (1997).
[11] The LFMR features discussed here are generic and not specific to its precise definition.
[12] M. Venkatesan *et al.*, J. Mater. Chem. **12**, 2184 (2002).
[13] J. M. D. Coey, J. Appl. Phys. **85**, 5576 (1999).
[14] J. M. D. Coey *et al.*, Phys. Rev. Lett. **80**, 3815 (1998).
[15] X. W. Li, A. Gupta, G. Xiao, and G. Q. Gong, Appl. Phys. Lett. **71**, 1124 (1997).
[16] J. Q. Xiao, J. S. Jiang, and C. L. Chien, Phys. Rev. Lett. **68**, 3749 (1992).
[17] E. g., see the review by S. Maekawa, S. Takahashi, and H. Imamura, in *Spin Dependent Transport in Magnetic Nanostructures*, edited by S. Maekawa and T. Shinjo, Series on Advances in Condensed Matter Science (CRC Press, Taylor and Francis, London, 2002), pp. 143.
[18] P. Majumdar and P. B. Littlewood, Nature (London) **395**, 479 (1998).
[19] M. J. Calderon, L. Brey, and F. Guinea, Phys. Rev. B **60**, 6698 (1999).
[20] In this Letter we refer to ''Grain Boundary'' in a broader sense to include, in addition to physical intergrain regions, any ''skin'' layer on the surface of the grains themselves, which might have a different magnetic property due to depolarization.
[21] P. W. Anderson and H. Hasegawa, Phys. Rev. **100**, 675 (1955).
[22] B. Kramer and A. Mackinnon, Rep. Prog. Phys. **56**, 1469 (1993).
[23] Our experimental results for MR(H, T) at all other temperatures (50 K, 100 K and 200 K), showing the same generic features as the 20 K data, appear to scale as MR(H/T) in conformity with calculated results.
[24] Preliminary simulations, where the grain spins have an explicit ferromagnetic exchange, and the antisite spins a strong magnetic anisotropy, and all updated via Monte Carlo, establish that one can theoretically reproduce the hysteresis of the magnetization also (see inset of Fig. 3(d)), which can be different from the MR, while retaining all the other features reported in Fig. 3.